Available online at www.sciencedirect.com

ScienceDirect

Procedia Manufacturing 00 (2019) 000–000

Procedia MANUFACTURING

www.elsevier.com/locate/procedia

23rd International Conference on Material Forming (ESAFORM 2020)

Development of a Modified Tool System for Lateral Angular Co-Extrusion to Improve the Quality of Hybrid Profiles

Bernd-Arno Behrens[a], Johanna Uhe[a], Susanne Elisabeth Thürer[b], Christian Klose[b] and Norman Heimes[a,*]

[a]*Institut für Umformtechnik und Umformmaschinen (Forming Technology and Forming Machines), Leibniz Universität Hannover, An der Universität 2, Garbsen 30823, Germany*

[b]*Institut für Werkstoffkunde(Materials Science), Leibniz Universität Hannover, An der Universität 2, Garbsen 30823, Germany*

* Corresponding author. Tel.: +49-511-762-2451; fax: +49-511-762-3007. *E-mail address:* heimes@ifum.uni-hannover.de

Abstract

The application of monomaterials is limited in lightweight construction concepts, because in addition to the weight requirements, the thermal and mechanical demands are constantly increasing. In order to ensure that the right material is used in the right place, the Collaborative Research Centre (CRC) 1153 is concerned with research into innovative process chains that lead to components with locally adapted properties. The lateral angular co-extrusion approach (LACE) allows the manufacturing of hybrid semi-finished products from aluminium alloy EN AW-6082 and steel AISI 5120. Throughout the LACE process, the steel tube is inserted into the extrusion die at an angle of 90° to the pressing direction, where it is covered in aluminium. The coaxial semi-finished products are subsequently formed into a hybrid bearing bushing by die forging. In this study, the LACE process is investigated on an industrial scale using a 10 MN extrusion press. The investigations are carried out by means of finite element (FE) simulation and are validated by a comparison with experimental results. The focus of this study is on the design and improvement of the aluminium material flow. The two major challenges of hybrid profile extrusion are the straightness of the extruded profile and, particularly in this study, the coaxial position of the support element. Within the numerical design process, different mandrel positions and chamber geometries are considered in terms of their influence on the profile quality. The numerically determined tool geometries are subsequently used for experimental investigations using the 10 MN extrusion press. The extruded hybrid profiles are compared with results of the numerical simulations. For the validation of the numerical model, metallographic analyses of the hybrid profiles as well as experimental extrusion force-time curves are used. Based on these results, the final mandrel position and chamber geometries are chosen and serve as a basis for further co-extrusion experiments.

Keywords: Co-Extrusion; Finite Element (FE) Simulation; Aluminium; Steel; Hybrid Profile

1. Introduction

The reduction of CO_2 emissions leads to a restriction of the application range of monomaterials in lightweight construction, since demands on high mechanical strength and high-temperature strength are increasing in addition to weight requirement [1]. Manufacturing components made of two different materials becomes more frepuent in order to achieve a greater reduction in weight. The production of hybrid components is already state of the art, however, the bond is usually only achieved during or after the forming process, whereby the joining zone can only be influenced by a subsequent process step [2]. The production of continuously reinforced semi-finished products is already state of the art using extrusion processes. However, either both the matrix and the reinforcing material are formed or there is no continuous feeding of the reinforcing element.

Foydl et al. used prepared billets with local reinforcements to produce hybrid profiles which were further processed by die forging [3]. The preparation of the extrusion billets is very complex and the reinforcing elements are not continuously in place. Weidenmann et al. developed an extrusion process with continuous feeding of several wires [4]. However, the reinforcement content was rather low due to the thin wires.

The Collaborative Research Centre (CRC) 1153 deals with novel process chains in which the joining process is carried out before the forming process. In one of the process chains, hybrid semi-finished products are produced using a lateral angular co-extrusion approach (LACE). The extruded semi-finished product consists of a coaxial composite of aluminium and steel. Here, the aluminium envelops the steel reinforcing element. Subsequently, the coaxial semi-finished products are formed to a hybrid bearing bushing by die forging.

Behrens et al. developed a laboratory-scale co-extrusion process for the 2.5 MN press numerically and experimentally [5]. Co-extrusion experiments on the laboratory scale were carried out to efficiently detect the influences of the process parameters and to minimise the costs for tools and materials. A round steel rod was fed into welding chamber of the porthole die perpendicular to the pressing direction of the aluminium alloy. In the welding chamber of the die, the steel rod was covered with aluminium and the hybrid profile exited the tool on the opposite side. Previous numerical investigations enabled a detailed understanding of the co-extrusion process [5, 6]. The hybrid profiles showed good bonding quality, which was proven by push-out tests. In addition, the quality of the longitudinal weld seams was tested using micro tensile specimens. Here, failure of the specimens occurred in the matrix material and not in the longitudinal weld seam [7]. The mechanical properties of the hybrid semi-finished products are therefore not critical for subsequent processes. However, Behrens et al. concluded that the observed non-coaxial position of the steel reinforcing element leads to problems in the following forging process [5].

The development of an extrusion tool for near-industrial scale experiments was then carried out based on the results of the previous laboratory tests. Thereby the boundary conditions of the laboratory process were maintained, as they led to sufficient mechanical properties of the hybrid semi-finished product. In addition to size scaling, the focus was on optimisation of the coaxial position of the reinforcing element and the geometrical shape tolerance of the profile. In this article, the new tool concept is introduced and the results of the experimental and numerical investigations for the development of the tool geometry are presented and compared.

2. Numerical Investigations

The new tool system for the 10 MN extrusion press at the Institute of Materials Science was derived from the smaller die used with the 2.5 MN press. A comparison of the size scaling of the semi-finished products obtained with both the 2.5 MN press and the 10 MN press is shown in Table 1.

The FE-model of the co-extrusion process was modelled and calculated in the commercial FEA-system FORGE NxT2.1. The 3D-FE-model contains 1.455.157 tetrahedral volume elements. The numerical model of the 10 MN process was set up based on the previously examined boundary conditions of the 2.5 MN process, which showed a good agreement with the experimental results. Coefficients of friction, heat transfer coefficients, contact conditions, material data and meshing settings were used as described in [7].

Table 1. Size scaling of the profile geometries from 2.5 MN to 10 MN press

Name	2.5 MN	10 MN
	Value in mm	Value in mm
Billet length	180	300
Billet diameter	56	142
Steel rod length	500	660
Steel rod/tube external diameter	15.2	38.0 / 44.5
Steel rod/tube internal diameter	-	32

Z-x symmetry is used to reduce model size and computational costs of this numerically challenging process. The main challenges in modelling the process are the self-contact of the aluminium and the use of two deformable parts. The tools were defined as rigid bodies, whereas the aluminium billet and the steel tube were modelled as deformable bodies. The temperature of the tools was constantly defined as T_{Tool} = 490 °C. The aluminium was homogeneously heated to T_{Alu} = 530 °C and the reinforcing element to T_{Steel} = 300 °C defined as bodies with heat conduction. As extrusion speed, a constant ram speed of 1 mm/s was used. Since thin-walled components cause a very high meshing effort, the steel tube is modelled as a steel rod in the simulation as a first approach to reduce the simulation time.

The geometric structure of the tool is shown in the cross section in Fig. 1. The aluminium billet is divided into two metal streams by the bridge and pressed through the press ram into the chamber die, which consists of two housing halves. Thereby the extrusion ram continuously increases the press height (p_h) and thus, reduces the length of the aluminium billet. The modularly constructed and separable chamber die consists of two housing halves, which are connected by dowel pins, keyways and screws.

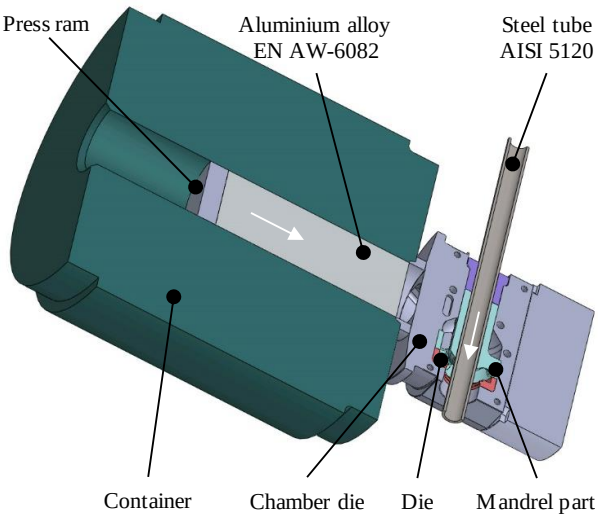

Fig. 1. Cross-section of the 10 MN tool system

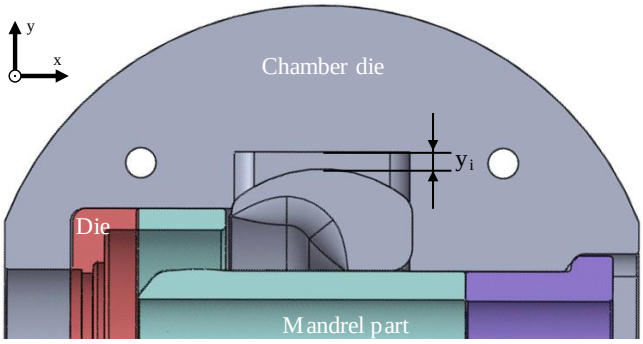

Fig. 2. Cross-section of the chamber die with cavity depth y_i

Preliminary extrusion tests resulted in extremely bent profiles due to the difference between the extrusion speeds of the two main metal streams. Hence, a pill-shaped cavity was milled into each half of the chamber die in order to decelerate the material flow and synchronize the metal streams depending on the cavity depth y_i, see Fig. 2.

As a reinforcing element, the steel tube is inserted into the welding chamber at an angle of 90° to the extrusion direction. Feeding and positioning of the steel tube is ensured by the mandrel element. Moreover, tilting of the reinforcement is avoided. The three support arms of the mandrel part divide the material flow once again and guide the divided aluminium streams into the antechamber of the die, which also acts as a welding chamber. Here, the individual metal streams are finally joined and onto the steel tube simultaneously. The outer diameter of the coaxial hybrid profile is determined by the internal die diameter of the die bearing.

Fig. 3 only shows the material flow of aluminium and the steel tube according to the previously described characteristic process stages. First, the aluminium is divided into two streams when it passes the portholes, Fig. 3b. The billet material flows further into the chamber, filling the side cavities and beginning to enclose the mandrel part, Fig. 3c. The three support arms of the mandrel part, whose position is clearly visible as a hole left of the pocket, then divide the material briefly into four separate streams, Fig. 3d. After filling the antechamber, the split aluminium streams touch the reinforcing element, and thus, the quasi-stationary phase of the process is initiated during which the aluminium pulls the steel tube out of the tool.

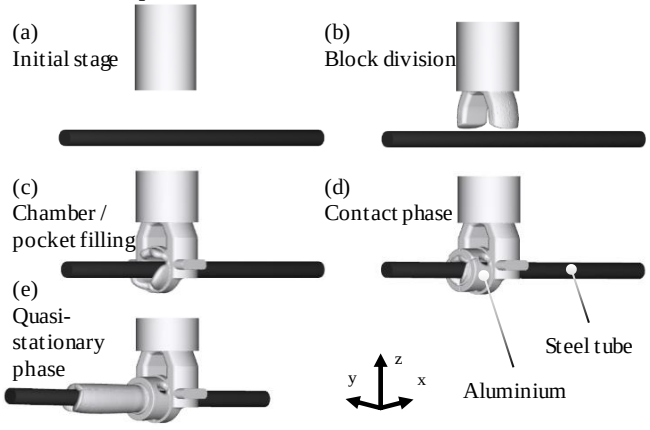

Fig. 3. Material flow of 10 MN process (a) press height (p_h) 0 mm, (b) p_h 39.5 mm. (c) p_h 85.5 mm (d) p_h 91.5 mm and (e) p_h 123.5 mm

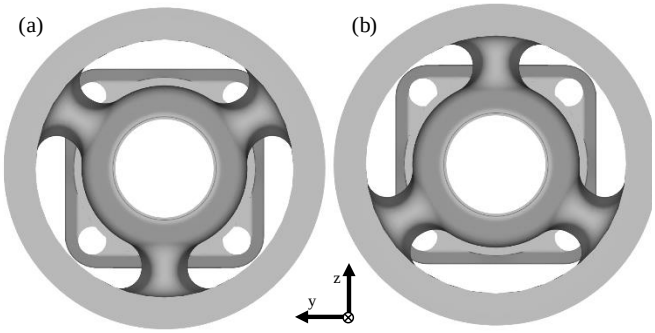

Fig. 4. Assembly positions of the mandrel (a) position A and (b) position variant B

With the new tooling system, an important role is assigned to the mandrel part. By positioning the reinforcing element, various assembly options can be realized due to the arrangement of the three support arms. Fig. 4 shows the two installation options which will be examined. The variants A (Fig. 4a) and B (Fig. 4b) each cause a different aluminium flow, whose influence on the profile geometry is to be determined. The positioning of the mandrel part was investigated numerically by using a pocket depth of 5 mm. These results are shown in Fig. 5.

For variant A, it is noticeable that the profile leaves the tool very straight. The difference of the aluminium streams in x-direction is named Δx_I. The aluminium streams are almost at the same height, which is confirmed by the low Δx_A. Only the lower string runs slightly ahead, which means that the steel rod is slightly inclined in the positive z-direction. In assembly position B, the upper aluminium string is fast forward, so that the rod in the mandrel section tilts strongly in the negative z-direction, see Fig. 5b. The tilting is clearly visible at the inclined end of the rod, and Δx_B is also significantly larger than Δx_A. The difference between the aluminium streams has an influence on the straightness of the profile.

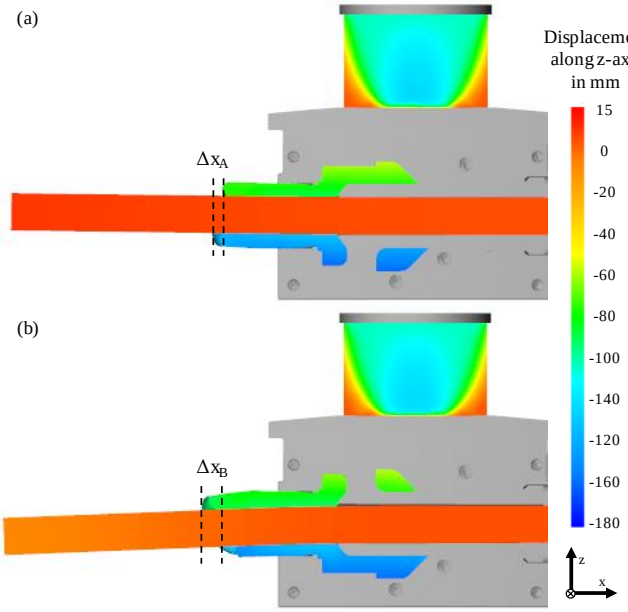

Fig. 5.Material flow and displacement in z-direction at a p_h of 105.5 mm (a) variant A (b) variant B

Due to the non-synchronized material flow in variant B, the streams encounter the steel rod at different times. This causes the steel rod to tilt to one side and the profile loses its straightness. Since the difference in A is much smaller than in B, the installation variant A is used for further investigations. In addition both illustrations in Fig. 5 show very clearly that dead zones typical for non-lubricant direct extrusion processes, which are characterized by almost no negative displacement in the z-direction, form at the front side of the billet in the contact zone between the aluminium alloy, the porthole die, and the recipient's inner lining. The displacement increases at the front of the aluminium billet, which is due to the material division and the formation of the string that is fed into the chamber.

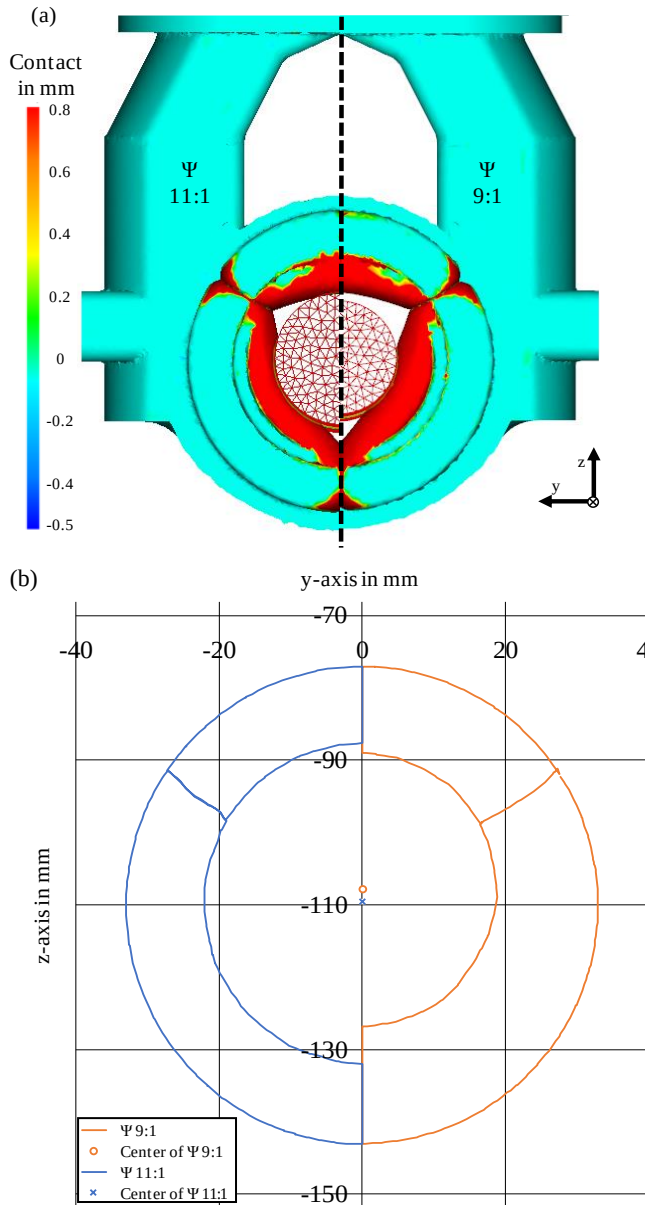

Fig. 6. (a) Stage of contact from the aluminium to the steel rod at a p_h of 89.5 mm left Ψ of 11:1 and right Ψ of 9:1, (b) cross-section of the profile at a p_h of 109.5 mm

Being able to realise co-extrusion processes with customisable reinforcement ratios allows for a possible increase of the range of application of such hybrid profiles. Specifically for the LACE process, variation of the steel tube's external diameters is considered in order to adjust the reinforcement ratio. This leads, to a different extrusion ratios simultaneously. For each extrusion ratio, different mandrel parts with the appropriate inner diameter are required. In this article, the extrusion ratios (ψ) for steel tubes with an external diameter of both Ø 44.5 mm and Ø 38 mm will be discussed. The extrusion ratio ψ is calculated as a ratio of the cross-sectional area of the upset aluminium billet in the container to the annular area of the extruded aluminium in the die. By using different tube diameters, the size of the annular area can be varied. The respective diameters of the steel tube considered here result in a Ψ of 11:1 and 9:1. The mandrel parts are assembled in installation variant A and the cavity depth y_i of the die housing is set to 5 mm. Fig. 6 shows the contact or distance to the nearest surface from the nodes of the aluminium alloy. The initial contact between the aluminium streams and the steel rod occurs at a press stroke of 89.5 mm. Fig. 6a shows the contact for an extrusion ratio Ψ of 11:1 and Ψ of 9:1 for comparison. It is noticeable that for the Ψ of 11:1, both streams come into contact almost simultaneously and thus only a slight tilting of the steel rod occurs. For a Ψ of 9:1, the lower string is well ahead of the upper string, which can be clearly seen from the gap between the steel rod and the upper string. In the further course of the process, the lower string will continue to push the steel rod towards the upper string until it comes into contact. Therefore, with an extrusion ratio Ψ of 9:1, a greater eccentricity is to be expected. This hypothesis is supported by the numerically calculated cross-sections of the profiles with extrusion ratios Ψ of 11:1 and 9:1, Fig. 6b. The cross-sections were plotted at a press stroke of 109.5 mm shortly after leaving the tool. For a Ψ of 11:1, the steel rod is almost coaxially in the centre at z-110 mm, whereas the steel rod has an eccentricity of almost 2 mm for a Ψ of 9:1.

The die housing is particularly characterised by its pocket geometry, which is intended to influence the material flow in a targeted manner. Fig. 2 shows a sectional view of the die housing. By varying the cavity depth, the volume that has to be filled by the aluminium streams varies. As a result, the aluminium enters the welding chamber at different times, so that the eccentricity of the reinforcing element can be minimised. The cavity depth y_i is varied uniformly as listed in Table 2.

Table 2. Variation of the pocket depth y_i

Pocket depth y_i	y_0	y_5	y_{10}
Value of y_i in mm	0	5	10

The numerical results for the different pocket depths are shown in Fig. 7. There, similar to Fig. 6b, the cross sections are plotted at a press stroke of 109.5 mm shortly after the profile has left the tool. The variation of y_i therefore has no influence on the eccentricity and the position of the reinforcement element for a Ψ of 9:1. Since a coaxial position could be achieved for the extrusion ratio of 11:1, a cavity depth of 5 mm is planned for the subsequent experimental investigations.

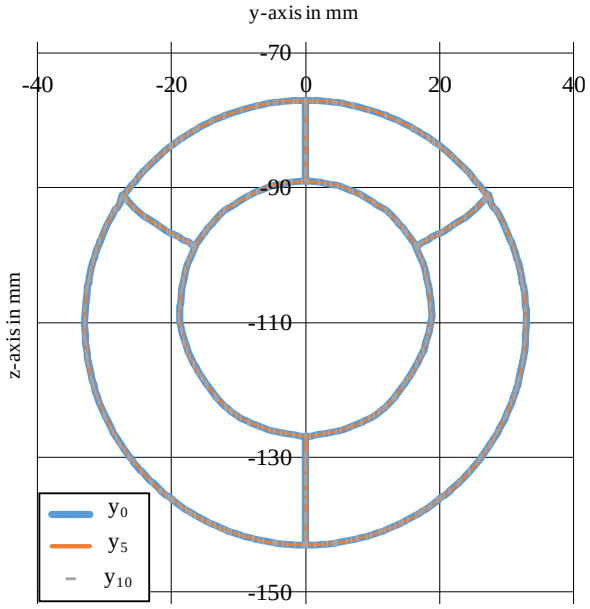

Fig. 7. Cross-section of the profile with a Ψ of 9:1 at a p_h of 109.5 mm for y_0, y_5 and y_{10}

3. Experimental Procedure

The experimental investigations were carried out based on the result of the numerical investigations. The components were heated homogeneously as per simulation and the tools were homogeneously heated as well prior to the tests. Assembly variant A of the mandrel part was used which showed the best results in the simulations. The toolkit was manufactured to fit the 10 MN extrusion press from SMS Meer and then employed for the extrusion tests at the Institute of Materials Science. In contrast to the simulation, a steel tube instead of a steel rod was used for these tests in order to allow for subsequent forging of hybrid bearing bushings from the extruded hybrid profiles. The cross sections shown in Fig. 8a-b indicate the position of the steel tube and the longitudinal weld seams in the actual hybrid profile. For better visualisation of the longitudinal weld seams, the cross sections were treated with H_2SO_4/HF etching solution. The cross section shown in Fig. 8a was taken from the profile that was extruded at a Ψ of 9:1. The slight eccentricity, which was observed in the simulation, is also apparent in the extruded profile. The cross section of the extrusion displayed in Fig. 8b, which was manufactured with a Ψ of 9:1, also corresponds to the numerical investigations. Fig. 8c shows the tip of the extruded aluminium alloy in hybrid profile from the back. It is clearly visible there that the lower aluminium string runs ahead. This observation is consistent with the results of the numerical investigations on the material flow. Fig. 8d shows a longitudinal section of the extruded profile for a Ψ of 11:1. The profile is very straight, which correlates with the coaxial position of the reinforcement. Moreover, the profile shows no overall significant diameter changes or waviness. Close contact between the aluminium alloy and the steel tube is present throughout the entire length and no microscopic gaps were observed.

For further validation, the geometries from the simulation are compared with the manufactured semi-finished products. The cross sections shown in Fig. 9 were taken after reaching a press height p_h of 109.5 mm, which corresponded with the position taken from the simulation. Four longitudinal weld seams, which are designated L_1-L_4 according to Fig. 9a, are visible. They result from the individual metal streams inside the tool, dividing the profile into four segments of two different sizes. The support arms of the mandrel part form the longitudinal weld seams L_1-L_3.

The longitudinal weld seam L_4 is formed as the aluminium streams, which were separated by the portholes, join prior to touching the steel reinforcement. The numerically determined position of the steel tube corresponds to the position in the real component, for Ψ 11:1 Fig. 9a and for Ψ 9:1 in Fig. 9b. In addition, the positions of the longitudinal weld seams are calculated with sufficient accurately by the FE simulation.

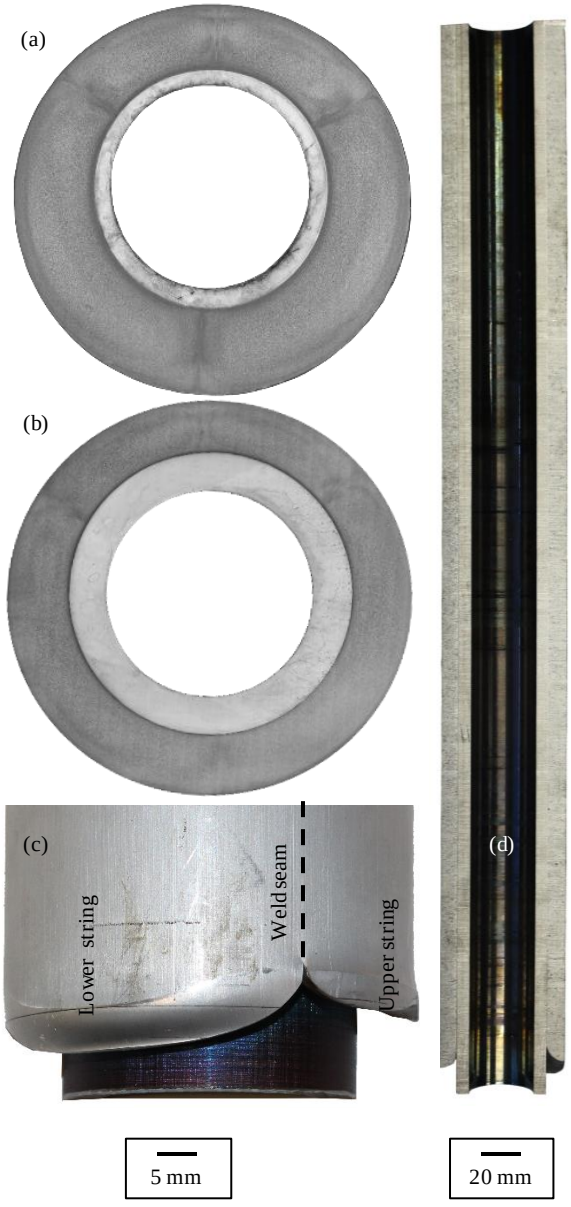

Fig. 8. (a) cross-section at p_h of 109.5 mm Ψ of 9:1, (b) cross-section at p_h of 109.5 mm Ψ of 11:1, (c) back of the beginning of the string Ψ of 11:1 and (d) cross-section along the length of the profile Ψ of 11:1

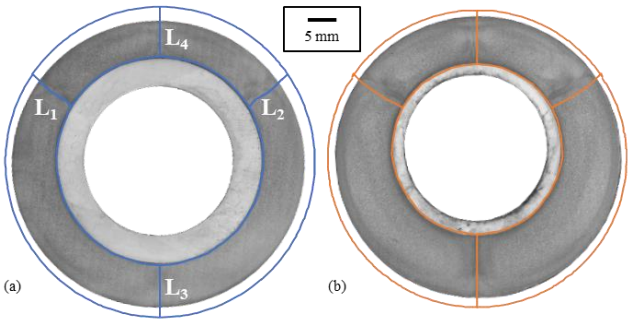

Fig. 9. Comparison of the geometries in the cross-section at a p_h of 109.5 mm (a) Ψ of 11:1 and (b) Ψ of 9:1

However, there is greater consistency between simulation and experiment for the positions of the longitudinal weld seams L_1 and L_3, indicated in Fig. 9a. The simulated geometry is slightly larger in diameter compared with the real component at both extrusion ratios, which can be explained by the intense deformations of the elements, which spring back more due to the self-contacting. Another reason for the deviation between the diameters might be related to the billet temperature, as the geometry of the simulation was exported at approx. 440 °C. However, the images of the semi-finished products were taken at room temperature condition. The rising of the aluminium can be reduced with finer meshing, but this will further increase the already high computing times. Furthermore, shrinkage can be taken into account by means of a downstream cooling simulation

In order to further evaluate the quality of the numerical results, the force-time curve of the simulation was compared to the experimentally recorded data. These results are shown in Fig. 10. The force progressions for both simulation and experiment show a similar course. In the experiment, it was not possible to operate at a constant pressing speed, because otherwise the aluminium billet temperature would have dropped too quickly. Furthermore, ram speed is manually regulated by a potentiometer. This results in a velocity profile that is kept approximately constant only in the quasi-stationary phase. Due to the different ram speeds, there is also a time shift. In order to minimise the time shift, the experimental velocity profile was approximated in a further step, Fig. 11 and implemented in the simulation as a boundary condition.

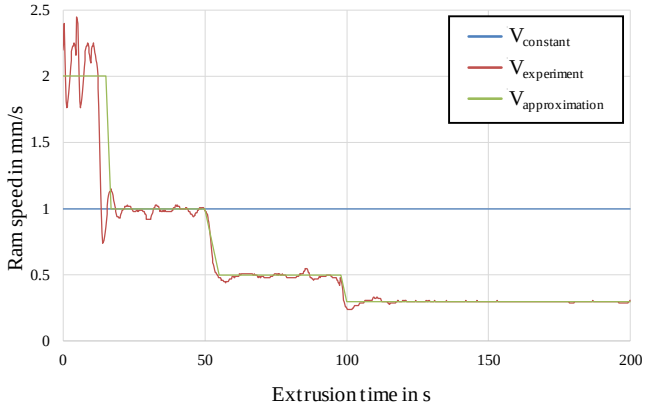

Fig. 10. Experimental and numerical velocity profile

The simulated force-time curve employing the approximated velocity profile is plotted as a dashed line in Fig. 10. While a small temporal difference remains due to the approximation of the experimentally recorded velocity profile, there is now much better consistency in the overall progressions of the simulated and experimental force curves.

Nevertheless, the curves show a high general degree of agreement, especially with regard to the maximum force in the quasi-stationary process area. In particular, the force curve progression exhibits several increases and plateaus that reflect the different characteristic process stages. First, the upsetting of the billet inside the container and the separation of the aluminium streams by means of the portholes cause a rapid force increase of the extrusion force. In the second area, the aluminium streams flow into the chamber and simultaneously fill the pockets. Due to further subdivision of the streams flowing by the support arms of the mandrel, as well as subsequent filling of the antechamber up to the point of contact between aluminium and the steel tube, the force increases continuously. In the following quasi-stationary phase, the force level remains approximately constant as the extruded profile is now continuously pressed out of the tool. The good agreement between numerical and experimental results in the quasi-stationary area confirms the initial assumption of the coefficient of friction of m = 0.95. This also corresponds to the coefficients of friction specified for the extrusion of aluminium in the literature [8, 9]. In the numerical simulation, the noise in the quasi-stationary area of the force progression curve is caused by the high coefficient of friction and the self-contact in the area of the longitudinal weld seams.

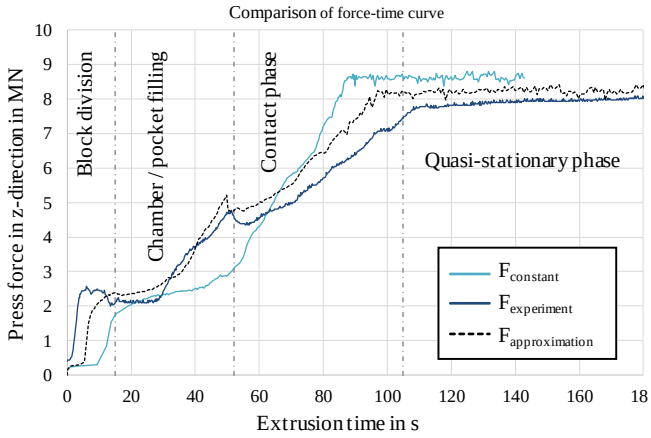

Fig. 11. Comparison of the experimental and numerical force-time curves

4. Summary and Outlook

A novel tool concept for the near-industrial scale co-extrusion of aluminium and steel using a LACE process was developed and subsequently validated by experimental results. Significant geometrical changes were made to the new tool concept compared with the previous laboratory-scale process and the planned improvements were named. By using a separate mandrel part, the steel tube reinforcement could be kept coaxial in the centre of the profile. A FE-model for the LACE process using the 10 MN extrusion press was built up and validated by experimentally determined data. The settings of the boundary conditions examined by Behrens et al. [6]

delivered very good and reproducible results. The simulated contour could be compared with the actual extruded profiles, which revealed good agreement between numerical and experimental results. It was further determined that different orientations of the mandrel's support arms inside the tool wield major influence on profile straightness. By contrast, variation of the depth of cavities inside the tool use for deceleration of the metal stings did not significantly influence the profile straightness.

In the future, further tests with adjusted process parameters will be carried out. In addition, it should be investigated numerically how reasonable coaxiality can be achieved at a Ψ of 9:1 by means of constructive alterations of the tool. Finally, the LACE process shall be transferred to more complex profile geometries such as asymmetrical hybrid profiles by employing a similar combined development process.

Acknowledgements

The results presented in this paper were obtained within the Collaborative Research Centre 1153 "Process chain to produce hybrid high performance components by Tailored Forming"-252662854 in the subproject A1. The authors would like to thank the German Research Foundation (DFG) for the financial support of this project.

References

[1] Hirsch J. Aluminium in innovative lightweight car design. Mater, Trans. 2011;52,:818–824.

[2] Groche P, Wohletz S, Brenneis M, Pabst C, Resch F. Joining by forming—A review on joint mechanisms, applicationsand future trends. Journal of Materials Processing Technology 2014;214:1972–1994

[3] Foydl A, Pfeiffer I, Kammler M, Pietzka D, Matthias T, Jäger A, Tekkaya AE, Behrens BA. Manufacturing of Steel-reinforced Aluminium Products by Combining Hot Extrusion and Closed-Die Forging. Key Engineering Materials 2012;504-506:481-486

[4] Weidenmann KA, Schomäcker M, Kerscher E, Löhe D, Kleiner M. Composite Extrusion of Aluminium Matrix Specimens Reinforced with Continuous Ceramics Fibres. Light Metal Age 2005;63

[5] Behrens BA, Klose C, Chugreev A, Thürer SE, Uhe J. Numerical investigations on the lateral angular co-extrusion of aluminium and steel. AIP Conference Proceedings 2018;1960:030001-1-030001-6

[6] Behrens BA, Klose C, Chugreev A, Heimes N, Thürer SE, Uhe J. A Numerical Study on Co-Extrusion to Produce Coaxial Aluminium-Steel Compounds with Longitudinal Weld Seams. Metals 2018;8(9):717

[7] Thürer SE, Uhe J, Golovko O, Bonk C, Bouguecha A, Behrens BA, Klose C. Mechanical Properties of Co-Extruded Aluminium-Steel Compounds. Key Engineering Materials 2017;742:512-519

[8] Chanda T, Zhou J, Duszczyk J. Application of three-dimensional numerical simulation to analysis of development of deformation zone at beginning of aluminium extrusion process. Mater. Sci. Technol. 2001;17:70–74

[9] Flitta I, Sheppard T. Nature of friction in extrusion process and its effect on material flow. Mater. Sci. Technol. 2013;19: 837–846